Effect of Ni Layer Thickness and Soldering Time on Intermetallic Compound Formation at the Interface between Molten Sn-3.5Ag and Ni/Cu Substrate

WON KYOUNG CHOI and HYUCK MO LEE

Department of Materials Science and Engineering, Korea Advanced Institute of Science and Technology, Kusung-Dong 373-1, Yusung-Gu, Taejon, Korea 305-701

The binary eutectic Sn-3.5wt.%Ag alloy was soldered on the Ni/Cu plate at 250°C, the thickness of the Ni layer changing from 0 through 2 and 4 μm to infinity, and soldering time changing from 30 to 120 s at intervals of 30 s. The infinite thickness was equivalent to the bare Ni plate. The morphology, composition and phase identification of the intermetallic compound (IMC, hereafter) formed at the interface were examined. Depending on the initial Ni thickness, different IMC phases were observed at 30 s: Cu_6Sn_5 on bare Cu, metastable $NiSn_3$ + Ni_3Sn_4 on Ni(2 μm)/Cu, Ni_3Sn_4 on Ni(4 μm)/Cu, and Ni_3Sn + Ni_3Sn_4 on bare Ni. With increased soldering time, a Cu-Sn-based η-$(Cu_6Sn_5)_{1-x}Ni_x$ phase formed under the pre-formed Ni-Sn IMC layer both at 60 s in the Ni(2 μm)/Cu plate and at 90 s in the Ni(4 μm)/Cu plate. The two-layer IMC pattern remained thereafter. The wetting behavior of each joint was different and it may have resulted from the type of IMC formed on each plate. The thickness of the protective Ni layer over the Cu plate was found to be an important factor in determining the interfacial reaction and the wetting behavior.

Key words: Ni layer thickness, eutectic Sn-3.5wt.%Ag alloy, Ni-Cu substrate

INTRODUCTION

The lead-tin (Pb-Sn) solder alloy has been widely used as interconnection materials in electronic packaging due to low melting temperatures and good wetting behavior on several substrates such as Cu, Ag, Pd, and Au. However, due to environmental and health concerns, alternative solder alloys are needed to meet stringent environmental regulations, requirements for greater mechanical reliability, and higher temperature service environments in automobiles and in avionics systems.[1–3] The tin-silver (Sn-Ag) binary solder alloy is an attractive candidate system.[4,5] In addition, multicomponent alloys based on this binary have been suggested to decrease the melting temperature of eutectic Sn-Ag (221°C) for lower temperature applications.[6,7]

The Ni coating is commonly used as a protective layer on a Cu conductor in electronic devices and circuit fabrications. It has interfaces with the Cu substrate and with the solder. However, there is no chemical reaction at the Cu interface and the IMC phase is not expected to form at this interface because the Cu-Ni binary system forms a complete solid solution. Thus, the existence of this interface is not detrimental to the solder joint reliability. In soldering, the molten solder reacts with the Ni layer first. The interfacial reaction is determined by the dissolution rate of Ni and the kind of IMC that has formed at the interface with the solder. The reaction of the solder on the Ni layer will be different from that on the Cu plate because its diffusivity is smaller than that of Cu.[8,9] With the increased soldering time, all of the Ni layer is supposed to be consumed and change into IMC and this will be affected by the layer thickness.

In this study, the binary eutectic Sn-3.5Ag was soldered on the Ni/Cu substrate with the Ni layer thickness (in μm) changing from zero through 2 and 4 to infinity. The zero and infinite thicknesses are equivalent to the pure Cu and Ni substrate, respectively. Through the change in layer thickness and soldering time, the interfacial reaction will be thoroughly investigated.

EXPERIMENTAL PROCEDURES

The solder alloy was prepared from pure metals (purity higher than 99.9%). Samples were encapsulated in quartz tubes under vacuum, melted, and held

(Received February 8, 1999; accepted April 7, 1999)

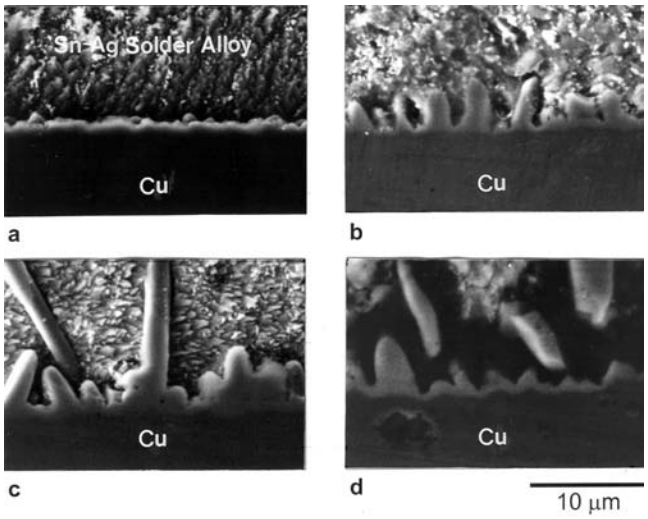

Fig. 1. Back-scattered SEM micrographs showing the interface of the Sn-3.5Ag/Cu plate when soldered for (a) 30 s; (b) 60 s; (c) 90 s; and (d) 120 s.

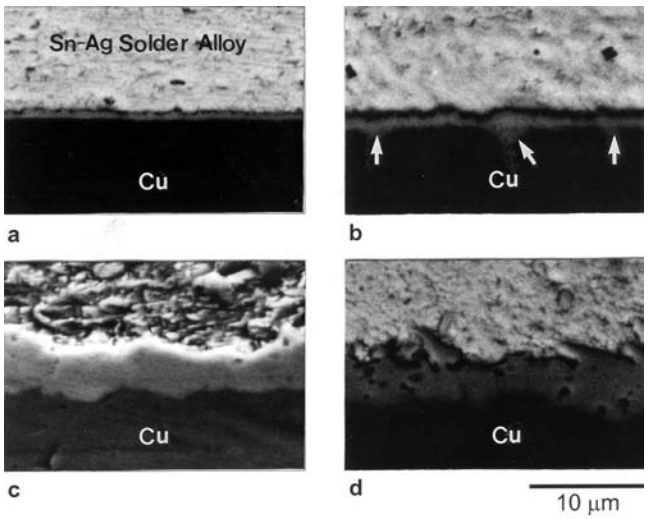

Fig. 2. Back-scattered SEM micrographs showing the interface of the Sn3.5Ag/Ni(2 μm)/Cu plate when soldered for (a) 30 s; (b) 60 s; (c) 90 s; and (d) 120 s.

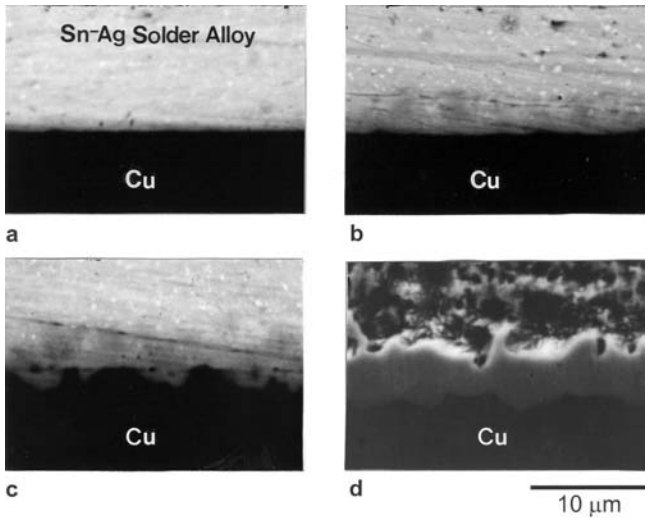

Fig. 3. Back-scattered SEM micrographs showing the interface of the Sn3.5Ag/Ni(4 μm)/Cu plate when soldered for (a) 30 s; (b) 60 s; (c) 90 s; and (d) 120 s.

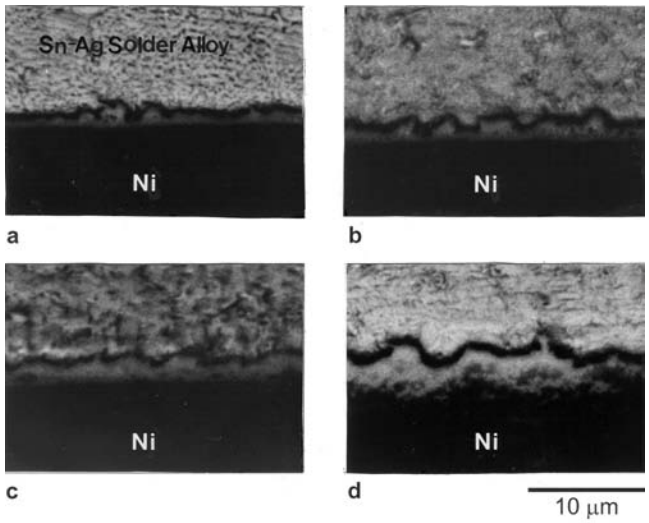

Fig. 4. Back-scattered SEM micrographs showing the interface of the Sn-3.5Ag/Ni when soldered for (a) 30 s; (b) 60 s; (c) 90 s; and (d) 120 s.

at 800°C for 30 min for mechanical mixing. As-cast alloys were made by cooling each melt into water. Then, they were cold-rolled into a 0.1 mm thick sheet and punched to a disk-type specimen (3 mm in diameter, 0.3 g).

Soldering was performed in the molten state at 250°C for 30 s, 60 s, 90 s, and 120 s using rosin mildly activated (RMA) flux to observe the growth behavior of IMCs. The oxygen free high conductivity Cu plates (0.5 mm) and Ni plates (0.5 mm) were polished with 1 μm diamond, then cleaned with acetone and alcohol. The Ni layer was electroplated on the Cu plate and the plating was performed in a nickel sulfate solution (Degussa Corporation) at 65°C with a current density of 50 mA/cm^2. The layer thickness was calculated as 2 μm and 4μm according to the Faraday equation.[10]

The interface was examined by the scanning electron microscopy (SEM) operated at 20 kV. In order to observe clearly the morphology of IMC at the interface, the solder matrix was etched by the use of 5%HNO_3-3%HCl-92%CH_3OH solution for several seconds. The composition of IMC was measured by the energy-dispersive x-ray (EDX) analyses. The spatial resolution was 1 μm diameter area about the target point and compositions were determined by an average of ten center point measurements. Its distribution through the joint was examined using the line scanning EDX analyses. The phases at the interface were identified by the x-ray diffraction (XRD) analyses. The specimens for XRD were prepared by mechanically removing the solder and etching away the remaining solder part with HCl solution for 30 s. Wetting tests were performed on a hot plate in air. The height of the spherical cap and wetting angle were directly measured from scanning electron micrographs (SEM) of the solder joints.

Table I. Composition (at.%) Change at the Interface Layer in Sn-3.5Ag Solder Joint with Soldering Time and Substrates.

Substrate	30 s	60 s	90 s	120 s
Cu plate	86Sn14Cu	58Sn42Cu	56Sn44Cu	52Sn48Cu
Ni(2 μm)/Cu plate	61Sn21Nil8Cu	65Sn25Ni10Cu 47Sn8Ni45Cu	67Sn23Ni10Cu 43Snl5Ni42Cu	64Sn25Ni11Cu 42Sn11Ni47Cu
Ni(4 μm)/Cu plate	46Sn42Ni12Cu	44Sn40Ni16Cu	61Sn31Ni8Cu 41Sn10Ni49Cu	52Sn33Ni15Cu 41Sn8Ni51Cu
Ni plate	14Sn86Ni	22Sn78Ni	22Sn78Ni	21Sn79Ni

RESULTS

The interface morphology of the Sn-3.5Ag alloy on the Cu plate, soldered at 250°C for 30 s through 120 s, is shown in Fig. 1a–d. Figure 2a–d represents the Ni(2 μm)/Cu plate under the same condition. In the latter case, the liquid solder reacts with the Ni layer and forms a first IMC probably composed of tin and nickel. Then, as the Ni layer is consumed by the interfacial reaction with the solder, the active Sn atoms in the liquid solder diffuse through the preformed Ni-Sn IMC layer and react with the Cu elements thereby forming a second scallop-type IMC composed mostly of copper and tin. It occurred at 60 s as marked by arrows in Fig. 2b.

The second IMC was observed at 90 s on the Ni(4 μm)/Cu plate as indicated in Fig. 3a–d. As the nickel layer was thicker than the previous case of Ni(2 μm)/Cu plate, it took longer for the tin to reach and react with the Cu substrate. The interfacial reaction for the bare Ni plate is represented in Fig. 4a–d. The second IMC did not exist because there was no copper in this bare Ni case.

To know the compositions of IMCs formed at the interface, the ten-average compositions of interfacial phases formed between the solder and the substrate were measured and recorded in Table I. They are regarded as approximate values because of the inherent measurement error range. For IMC on the bare Cu plate, the composition of Cu increases rapidly with increased soldering time and that of Sn decreases. Initially at 30 s, the tin content in the solder must have been included in the measurement because of the similar beam size (1 μm) of EDX relative to the thickness of the interface. For the Ni/Cu plate, irrespective of thickness, the interfacial region divides into two layers, Ni-Sn IMC at the top and Cu-Sn IMC underneath. The two-layer pattern occurred at 60s for the Ni(2 μm)/Cu plate and at 90 s for the Ni(4 μm)/Cu plate, which is consistent with observations of Figs. 2 and 3.

To identify the phase of IMC and also observe the effect of the thickness of Ni layer, the XRD analysis was performed. Figure 5 represents typical XRD patterns of the interface soldered at 250°C for 30 s. Excluding the solder element of Sn and the substrate elements of Cu and Ni which are also detected, only the η-Cu_6Sn_5 IMC was observed on the bare Cu plate. It was reported that the η-Cu_6Sn_5 phase formed at the interface between the Sn-3.5Ag solder and the Cu

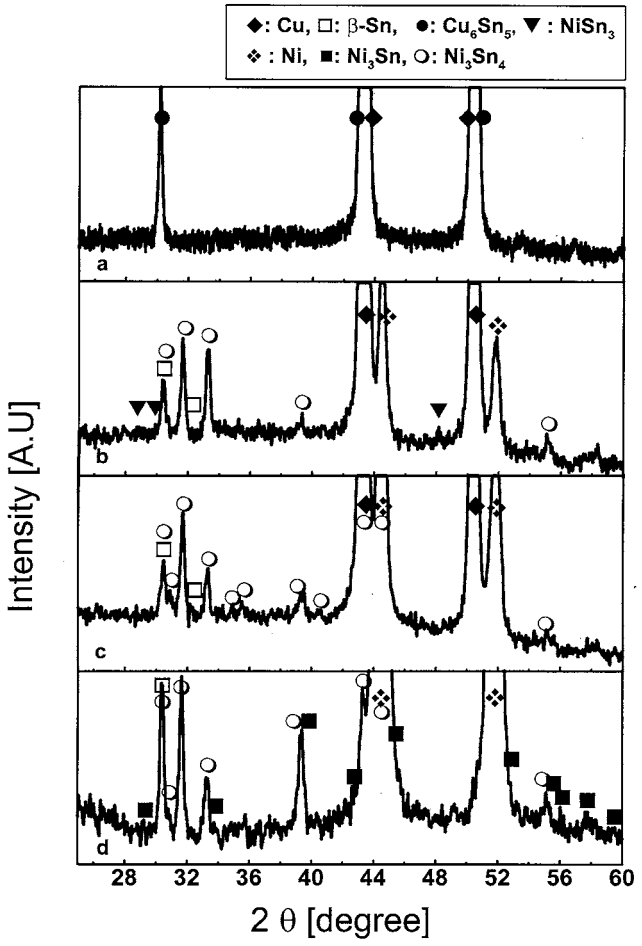

Fig. 5. XRD patterns of the interface in the solder/substrate joints after soldering at 250°C for 30 s: (a) Sn-3.5Ag/Cu plate; (b) Sn-3.5Ag/Ni(2 μm)/Cu plate; (c) Sn3.5Ag/Ni(4 μm)/Cu plate; and (d) Sn-3.5Ag/Ni plate.

plate in the liquid state soldering.[1,11–13] The ε-Cu_3Sn phase was observed below the η-Cu_6Sn_5 phase only at the solid state aging of elevated temperatures and prolonged time.[1,11,12] On the Ni(2 μm)/Cu plate, metastable $NiSn_3$ and stable Ni_3Sn_4 phases were detected while only Ni_3Sn_4 was observed on the Ni(4 μm)/Cu plate. The $NiSn_3$ is regarded as metastable.[14] On the Ni plate, two different phases of Ni_3Sn_4 and Ni_3Sn were identified. For the bare Ni plate, another Ni_3Sn_2 phase was detected at 60 s by XRD in addition to Ni_3Sn_4 and Ni_3Sn that were already present early at 30 s. This additional IMC did not disappear until

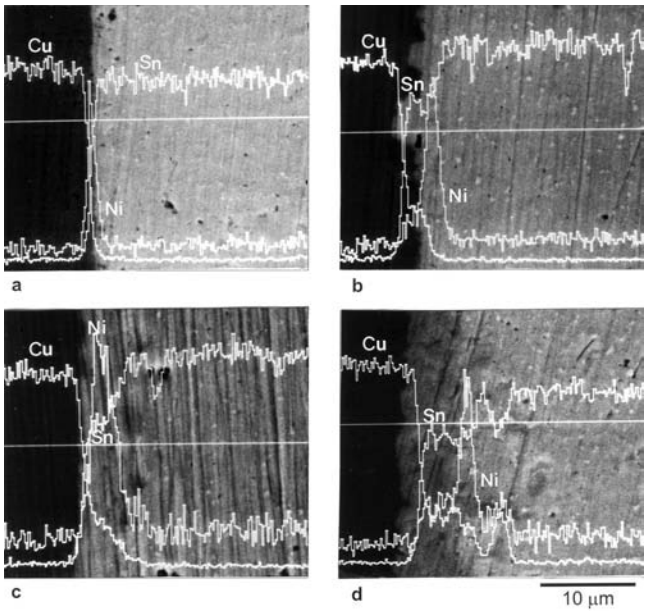

Fig. 6. Line-scanned SEM images of the interface in the Sn-3.5Ag/Ni(2 μm)/Cu joints when soldered for (a) 30 s; (b) 60 s; (c) 90 s; and (d) 120 s.

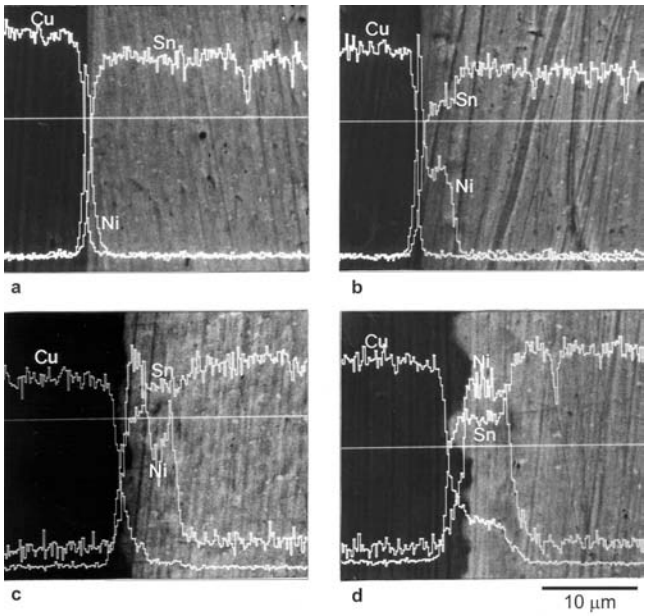

Fig. 7. Line-scanned SEM images of the interface in the Sn-3.5Ag/Ni(4 μm)/Cu joints when soldered for (a) 30 s; (b) 60 s; (c) 90 s; and (d) 120 s.

soldered for 120 s, thereby the IMC phases being a mixture of Ni_3Sn_4, Ni_3Sn_2, and Ni_3Sn from 60 s until 120 s.

The Ni-Sn layer seems to be monolithic in terms of morphology but it is composed of two or three different phases as confirmed by XRD. To check out in detail the compositions of IMCs formed at the interface, the interface was scanned. Figure 6a–d shows the line-scanned profile of each element of Sn, Ni, and Cu near the substrate interface in the Sn-Ag/Ni (2 μm)/Cu plate with increased soldering time while the Sn-Ag/Ni(4 μm)/Cu plate is shown in Fig. 7a–d. However, this analysis was not able to differentiate successfully the phases of the Ni-Sn IMC. In the case

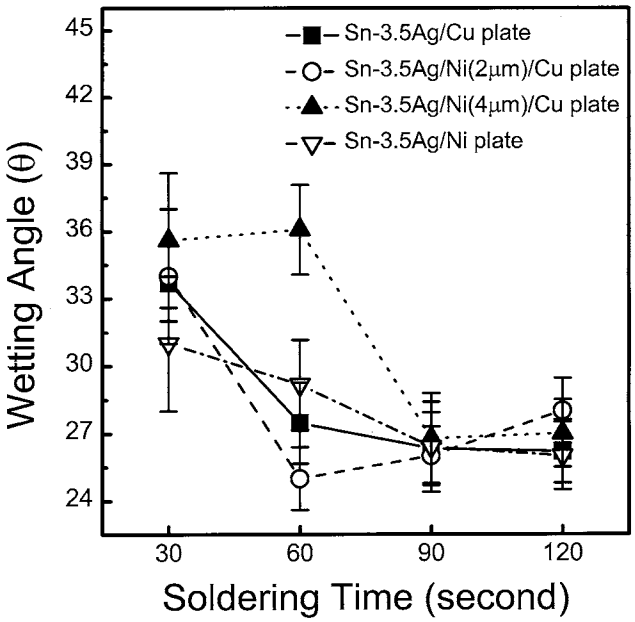

Fig. 8. Change of wetting angle with soldering time.

of the Ni(4 μm)/Cu plate at 30 s and 60 s, there is only one IMC layer of Ni_3Sn_4 between the solder and the Cu plate. After 90 s, the η-$(Cu_6Sn_5)_{1-x}Ni_x$ IMC is observable below the Ni-Sn IMC layer by compositions and morphology as seen in Figs. 3c,d and 7c,d.

Depending on the thickness of Ni layer and soldering time, different interfacial reactions occurred and different IMC phases formed. To relate interfacial phenomena with wetting behaviors, the wetting angle was measured with soldering time. According to Fig. 8, the wetting angle on the bare Cu plate decreases at a fast rate while it does at a slow rate on the bare Ni plate. An abrupt change in the wetting angle is noticeable between 30 s and 60 s for the Ni(2 μm)/Cu plate and between 60 s and 90 s for the Ni(4 μm)/Cu plate. It coincides with a formation of the two-layer IMC pattern for both plates.

DISCUSSION

The two-layer pattern such as the Ni-Sn IMC at top and Cu-Sn IMC underneath the Ni-Sn IMC was also observed when the solder paste of the same composition as in this work reacted with the Ni(2 μm)/Cu(2 μm) base.[15] What has been additionally observed in this study is that the nature of the Ni-Sn IMC is complicated. In the Ni-Sn binary system, there exist three stable intermediate phases, Ni_3Sn, Ni_3Sn_2, and Ni_3Sn_4. All the three phases were detected though at different soldering conditions. The metastable $NiSn_3$ was observed, too. The type of IMC phases formed at the interface followed the Ni-rich trend with the increased Ni layer thickness at least in the early soldering stage: $NiSn_3$ + Ni_3Sn_4 at 2 μm, Ni_3Sn_4 at 4 μm, and Ni_3Sn_4 + Ni_3Sn at infinity.

It has been reported that the apparently most stable Ni_3Sn_4 phase formed on the Sn-rich solder/Ni joint under various conditions.[16–20] A recent study by Bader et al.[21] found that both Ni_3Sn_4 and Ni_3Sn_2

formed at 300°C, however, the nucleation of the Ni_3Sn_4 phase was faster and its layer was much thicker. This may be the reason why Ni_3Sn_2 formed only after 60 s for the bare Ni plate in this work. Even if the metastable $NiSn_3$ phase was found in Sn and 63Sn-37Pb plating over Ni,[16] its presence was rarely reported. Nonetheless, previous studies are generally consistent with the current observation. The type of IMC phase first formed at the interface was predicted through thermodynamic calculations and successfully compared with experimental observations by Lee et al.[22] who used the driving force concept. When this approach was applied to the current ternary system of Sn-Ag-Ni using thermodynamic descriptions assessed by Ghosh,[23] the IMC phase with the largest driving force as well as the largest enthalpy of formation is calculated as not Ni_3Sn_4 but Ni_3Sn_2. As suggested by Chen et al.,[20] the difficulty of the formation of Ni_3Sn and Ni_3Sn_2 may be due to their nucleation difficulty and instability resulting from their mass transport properties.

The dissolution rate of Cu in the tin matrix is much faster than that of Ni at the soldering temperature of 250°C.[8,9,24] The fast dissolution rate of the substrate element into the solder enables the wetting angle of the solder onto the substrate to change fast.[25,26] This is the reason why the wetting angle of the Sn-3.5Ag solder on the bare Cu plate decreased fast while the wetting angle of the same solder on the bare Ni plate decreased relatively slowly with respect to time. An abrupt change in the wetting angle that was observed between 30 s and 60 s for the Ni(2 μm)/Cu plate and between 60 s and 90 s for the Ni(4 μm)/Cu plate matched with the appearance of the η-$(Cu_6Sn_5)_{1-x}Ni_x$ IMC phase under the Ni-Sn IMC layer for both plates. Kim[27] suggested that the wetting procedures were controlled by the surface energy balance among solder, substrate metal and interfacial IMC phase as well as the change in their Gibbs energy during soldering. The change of the interfacial IMCs brought an abrupt change in the wetting balance and the resultant change of the wetting angle as indicated in this study.

SUMMARY

As the thickness of the Ni layer over the Cu substrate increased, Ni-Sn-based and more Ni-rich IMC phases were found. The layer remained as a planar type though slightly rough and its growth was slow. With increased soldering time, the η-$(Cu_6Sn_5)_{1-x}Ni_x$ IMC formed as a scallop type below the pre-formed Ni-Sn IMC. The change of wetting angle was explained by different dissolution rates of Cu and Ni and the emergence of the Cu-Sn IMC layer below the Ni-Sn IMC layer.

ACKNOWLEDGEMENTS

This study has been supported by the Center for Interface Science and Engineering of Materials (CISEM) at KAIST and many discussions with Dr. S.W. Yoon at Hyundai Electronics are acknowledged.

REFERENCES

1. W. Yang, R.W. Messler, Jr., and L.E. Felton, *J. Electron. Mater.* 23, 765 (1994).
2. S. Jin, *JOM* 45, 13 (1993).
3. S.W. Yoon, J.-R. Soh, B.-J. Lee, and H.M. Lee, *Acta Mater.* 45, 951 (1997).
4. C. Melton, *JOM* 45, 33 (1993).
5. J. Glazer, *J. Electron. Mater.* 23, 693 (1994).
6. M.E. Loomans, S. Vaynman, G. Ghosh, and M.E. Fine, *J. Electron. Mater.* 23, 741 (1994).
7. S.K. Kang and A.K. Sarkhel, *J. Electron. Mater.* 23, 701 (1994).
8. H.G. Schenzel and H. Kreye, *Plat. Surf. Finish.* 77, 50 (1990).
9. W.G. Bader, *Welding J., Res. Suppl.* 48, 551-s (1969).
10. M.G. Fontana, *Corrosion Engineering, 3rd ed.* (New York: McGraw-Hill, 1987).
11. P.T. Vianco, K.L. Eriksson, and P.L. Hopkins, *J. Electron. Mater.* 23, 721 (1994).
12. W. Yang, L.E. Felton, and R.W. Messler, Jr., *J. Electron. Mater.* 24, 1465 (1995).
13. H.K. Kim and K.N. Tu, *Phys. Rev.* 53B, 16027 (1996).
14. T.B. Massalski, *Binary Alloy Phase Diagrams, 2nd ed.* (Materials Park, OH: ASM, 1992).
15. S.K. Kang, R.S. Rai, and S. Purushothaman, *J. Electron. Mater.* 25, 1113 (1996).
16. J. Haimovich, *Welding J., Res. Suppl.* 8, 101-s (1989).
17. S.K. Kang and V. Ramachandran, *Scripta Metall.* 14, 421 (1980).
18. K.N. Tu and R. Rosenberg, *Jpn. J. Appl. Phys. Suppl.* 2, Part I, 633 (1974).
19. W.J. Tomlinson and H.G. Rhodes, *J. Mater. Sci.* 22, 1769 (1987).
20. S.-W. Chen, C.-M. Chen, and W.-C. Liu, *J. Electron. Mater.* 27, 1193 (1998).
21. S. Bader, W. Gust, and H. Hieber, *Acta Mater.* 43, 329 (1995).
22. B.-J. Lee, N.M. Hwang, and H.M. Lee, *Acta Mater.* 45, 1867 (1997).
23. G. Ghosh, *Metall. Mater. Trans.* 30A, 5 (1999).
24. C.H. Ma and R.A. Swalin, *Acta Metall.* 8, 388 (1960).
25. F.G. Yost, P.A. Sackinger, and E.J. O'Toole, *Acta Mater.* 46, 2329 (1998).
26. J.A. Warren, W.J. Boettinger, and A.R. Roosen, *Acta Mater.* 46, 3247 (1998).
27. H.K. Kim (Doctoral Thesis, University of California at Los Angeles, 1996).